Optimal Combined Seismic and Energy Efficiency Retrofitting for Existing Buildings in Italy

Nicholas Clemett[1]; Wilson Wladimir Carofilis Gallo[2]; Giammaria Gabbianelli[3]; Gerard J. O'Reilly[4]; and Ricardo Monteiro[5]

Abstract: A large portion of aging existing buildings are susceptible to significant structural damage during earthquakes and suffer from poor energy performance. When considering how to improve the seismic performance and energy efficiency of these structures, retrofitting has been shown to be a more attractive alternative compared to complete demolition and reconstruction. Not only is retrofitting generally preferable from an economic perspective, but it also typically has lower levels of social and environmental impact as well. Together, these three aspects (economic, social, and environmental) form the so-called three pillars of sustainability. Recently, research efforts have begun to focus on developments in combined and integrated seismic and energy retrofit frameworks and techniques, showing that investing in combined retrofitting schemes is often more cost effective than conducting either energy-efficiency or seismic retrofitting alone. As new national and transnational policies place greater emphasis on the environmental impact of the built environment, it is crucial that combined retrofit schemes be evaluated in a comprehensive manner that allows for the selection of optimal schemes when a range of key sustainability-related decision variables (DVs) are considered. This study investigated the selection of a life cycle assessment (LCA)-based optimal combination of seismic and energy-efficiency retrofit schemes for an existing reinforced concrete case-study building in Italy. The seismic performance of the retrofit schemes was evaluated using detailed nonlinear time-history analysis and the Pacific Earthquake Engineering Research Centre's performance-based earthquake engineering (PEER-PBEE) framework, and the resulting economic costs and environmental impacts were incorporated into the LCA methodology. A detailed energy assessment was performed for each retrofit scheme so that the costs and environmental impacts associated with the operation of the building could be included in the LCA. Subsequently, the characteristics of each retrofit scheme were evaluated for a range of additional DVs, which encompassed the three pillars of sustainability. Finally, a multicriteria decision-making process was used to evaluate the optimal combination of seismic and energy retrofit schemes for several locations exhibiting different combinations of seismicity and climatic conditions. The results of this study provide insight into which combinations of seismic and energy efficiency retrofit measures can produce optimal solutions within the constraints set by decision makers and illustrate how assessments of both seismic and energy retrofit interventions can be implemented in the future. **DOI: 10.1061/(ASCE)ST.1943-541X.0003500.**

Introduction

A significant portion of the Italian building stock was built in the years following the second world war, prior to the introduction of modern design codes (Asprone et al. 2013). It is well-documented that these aging buildings, which generally consist of RC moment-resisting frames (MRFs) with unreinforced masonry (URM) infills, are not only susceptible to significant structural damage during earthquakes but also suffer from poor energy efficiency due to aging materials, making them relatively expensive to operate and maintain energetically (Menna et al. 2021; Pohoryles et al. 2020). When seeking to improve the seismic and energy performance of deficient buildings, retrofitting of existing structures and external envelopes is generally preferred because it is more cost effective and has significantly lower impact on the environment than complete demolition and reconstruction.

The general aim of retrofitting is to address the critical deficiencies of a building and improve its performance. From a structural perspective, typical deficiencies of infilled RC MRFs include unreinforced joints, insufficient column shear capacity, low-ductility beams and columns, and the formation of soft-story mechanisms. A variety of structural retrofit measures (SRMs) are available to address these issues, including fiber-reinforced polymer (FRP) wrapping (Del Vecchio et al. 2015); joint enlargement (Karayannis et al. 2008); the introduction of new lateral load resisting systems, such as RC shear walls (Calvi 2013), steel braces (Mazzolani et al. 2018), or exoskeleton systems (Passoni et al. 2021); and the reduction of the seismic load through additional damping devices, such as fluid viscous dampers (Pettinga 2020) or base isolation (Calvi 2013).

Substandard energy performance can typically be attributed to the poor thermophysical characteristics of envelope elements,

[1]Postgraduate Researcher, Univ. School for Advanced Studies IUSS, Palazzo del Broletto, Piazza della Vittoria n.15, Pavia 27100, Italy; Postgraduate Researcher, Università degli Studi di Pavia, Facoltà di Ingegneria, Via Adolfo Ferrata n.5, Pavia 27100, Italy (corresponding author). ORCID: https://orcid.org/0000-0003-3733-4971. Email: nicholas.clemett@iusspavia.it

[2]Postgraduate Researcher, Univ. School for Advanced Studies IUSS, Palazzo del Broletto, Piazza della Vittoria n.15, Pavia 27100, Italy. Email: wilson.carofilis@iusspavia.it

[3]Postdoctoral Researcher, Univ. School for Advanced Studies IUSS, Palazzo del Broletto, Piazza della Vittoria n.15, Pavia 27100, Italy. ORCID: https://orcid.org/0000-0003-0657-9538. Email: giammaria.gabbianelli@iusspavia.it

[4]Assistant Professor, Univ. School for Advanced Studies IUSS, Palazzo del Broletto, Piazza della Vittoria n.15, Pavia 27100, Italy. ORCID: https://orcid.org/0000-0001-5497-030X. Email: gerard.oreilly@iusspavia.it

[5]Associate Professor, Univ. School for Advanced Studies IUSS, Palazzo del Broletto, Piazza della Vittoria n.15, Pavia 27100, Italy. ORCID: https://orcid.org/0000-0002-2505-2996. Email: ricardo.monteiro@iusspavia.it

Note. This manuscript was submitted on September 21, 2021; approved on July 13, 2022; published online on October 18, 2022. Discussion period open until March 18, 2023; separate discussions must be submitted for individual papers. This paper is part of the ***Journal of Structural Engineering***, © ASCE, ISSN 0733-9445.

such as poorly insulated walls, roofs, or windows; the presence of thermal bridges; insufficient exposure to the sun; or outdated and inefficient lighting, heating, and cooling systems (Evangelisti et al. 2015; Zinzi et al. 2016). Typical energy retrofit measures (ERMs) that can address these deficiencies include the installation of new insulation materials, either in the form of external insulation panels [such as expanded polystyrene (EPS)], loose-fill cavity insulation, or foam insulation products (Menna et al. 2021); the installation of high performance windows with insulated PVC frames, multiple glass layers covered with low emissivity coatings and low conductivity gases (Menna et al. 2021; Mora et al. 2018; Rosso et al. 2020); the replacement of existing light fixtures with high efficiency alternatives (Menna et al. 2021); the replacement of an existing heating and cooling plant with new energy efficient alternatives (Mauro et al. 2017; Menna et al. 2021; Mora et al. 2018).

Given the broad range of SRMs and ERMs available, there has been significant focus in recent years on developing methodologies that aim to determine optimal seismic or energy retrofit configurations for existing buildings. Various methods, such as index-based methods (Requena-García-Cruz et al. 2019), cost-benefit analyses (Cardone et al. 2019; Sousa and Monteiro 2018), and multicriteria decision making (MCDM) (Caterino et al. 2008; Gentile and Galasso 2019) have been used to select an optimal structural retrofit schemes from a finite range of possible alternatives. In addition, advanced optimization methods utilizing evolutionary algorithms have been employed to develop optimal designs for seismic or energy retrofit interventions considering both single-criterion and multicriteria optimizations (Di Trapani et al. 2020; Falcone et al. 2019; Mauro et al. 2017; Rosso et al. 2020). However, the aforementioned methodologies do not consider combined seismic and energy retrofitting in a single assessment. Currently, seismic assessment using these frameworks is limited to simplified procedures due to the extreme computational complexity involved in performing a large number of nonlinear time-history analyses (NLTHAs).

With the modern focus on developing sustainable solutions to design problems, it is important that decision support systems used to aid in the selection of optimal solutions accommodate not just technical or economic variables but also social and environmental variables. Economics, society, and the environment are the so-called three pillars of sustainable design (WCED 1987). Of the aforementioned decision support systems, the MCDM framework is the most comprehensive and flexible, and is capable of considering a broad range of decision variables (DVs). Recent studies have used this methodology to successfully select optimal seismic retrofit solutions for existing buildings while considering a selection of DVs from all three pillars of sustainability (Clemett et al. 2022; Passoni et al. 2021).

Historically, the need for seismic and energy retrofit interventions has been treated as two separate problems that have little influence on each other. However, studies have highlighted that the benefits achieved by thermal refurbishment of existing buildings can be significantly eroded if additional losses associated with seismic hazards are not taken into consideration (Mauro et al. 2017; Menna et al. 2019). To address this fact, recent studies have focused on retrofitting buildings to simultaneously improve their seismic and energy performance; however, these studies have tended to consider only one or two possible SRMs, such as new RC walls or FRP joint strengthening, in combination with a fixed set of ERMs (or vice versa) instead of a range of feasible alternatives (Caruso et al. 2020); consider only one or two possible DVs, typically economic variables such as installation cost or total life-cycle cost instead of a range of economic, environmental, and social parameters that are key to ensuring a sustainable design (Formisano et al. 2019; Mora et al. 2018; Pohoryles et al. 2020; Sassu et al. 2017) or; use a decision support framework that can assist in aiding decision makers but stops short of providing concrete, rational recommendations for an optimal solution (Calvi 2013; Passoni et al. 2021).

The aim of the present study was to illustrate how a general and robust decision-making framework, such as MCDM, can be used to combine results from seismic and energy performance assessments and select, from a finite choice of alternatives, an overall optimal combined retrofit scheme while considering a broad range of economic, social, and environmental DVs. By assessing performance of the alternatives in three different locations across Italy, this study provides insights into how different combinations of seismic and climatic demands can affect the choice of an optimal retrofit combination solution.

Assessment and Selection Methodology

The methodology for assessing the performance of retrofit alternatives and selecting an optimal design comprised three primary phases: (1) seismic retrofit design and performance assessment; (2) energy retrofit design and performance assessment; and (3) MCDM assessment. In this study, it was assumed that the SRMs did not influence the energy performance of the buildings, and vice versa for the ERMs. This allowed the seismic and energy designs to be performed independently and the results combined in the final MCDM stage to determine DV values.

Seismic Design and Performance

The design of the SRMs was conducted in accordance with Italian building code norme tecniche per le costruzioni (NTC) (NTC 2018). Nonlinear static analysis, through the N2 method (Fajfar 2000), was used to identify critical structural weaknesses and the expected seismic performance of case-study structures as well as to check code requirements (drift limits, internal forces, etc.). The SRMs were designed to address these weaknesses and improve the performance of structures as much as possible, acknowledging that the performance achieved might not be equal to the performance required for new code-conforming buildings due to practical and financial considerations (Calvi 2013). This design approach was in line with the goals of recent risk-reduction programs, such as the Italian Sismabonus scheme (Cosenza et al. 2018). Following the design and preliminary assessment, a detailed seismic performance and loss assessment was performed utilizing NLTHA and the probabilistic Pacific Earthquake Engineering Research Centre's performance-based earthquake engineering (PEER-PBEE) methodology (FEMA 2018a). The loss calculations were performed using the PEER performance assessment and calculation tool (PACT) (FEMA 2018b). The primary output from the detailed seismic performance assessment was the expected annual loss (EAL), the expected annual environmental impacts (EAEI), and the annual probability of failure (APF), which were used to calculate the values of several of the DVs described in the following sections.

In this study, four different seismic retrofit schemes were considered: (1) S_1—local strengthening with carbon FRP (CFRP); (2) S_2—global strengthening with additional concentric steel braces; (3) S_3—CFRP strengthening combined with additional concentric steel braces; and (4) S_4—CFRP strengthening combined with additional viscous dampers. In addition, in all the SRMs, URM infill was separated from the RC frames by the provision of a seismic gap in order to eliminate column–infill interaction and reduce the shear forces acting on the columns. The primary intervention techniques used in each retrofit scheme are summarized in Table 1, while the design procedure for each of the SRMs and any associated assumptions are reported in previous studies by the authors (Carofilis et al. 2020; Clemett et al. 2022).

Table 1. Summary of the four seismic retrofit schemes considered in this study

Scheme	Interventions	Effect
S1	CFRP strips to BCJ	Increases joint shear resistance
	CFRP bars to columns	Increases column stiffness and flexural capacity
	CFRP wrap of columns and beams	Increases shear resistance of elements and confinement
S2	Exterior steel X-braces	Reduces force and displacement demand on MRF
S3	CFRP as for S1	—
	Braces as for S2	—
S4	CFRP as for S1	—
	Viscous dampers	Reduces displacement and acceleration demands

Table 2. Summary of the energy retrofit measures adopted for each of the three energy retrofit schemes

Scheme	Envelope ERMs	Plant/services ERMs
E1	External roof insulation with EPS panels	Replace fluorescent lights with efficient LEDs
		Install thermostatic valves on radiators
E2	E1 interventions +	
	External wall insulation with EPS panels	—
E3	E2 interventions +	
	Replacement of windows with new double or triple glazing with PVC frames and internal venetian blinds	Replace existing boiler with new high efficiency condensing boiler
		Install new lighting control systems
	Floor insulation (where required)	Install new photovoltaic panels on roof

Energy Performance

The energy performance of the case-study structure was assessed using the EDILCLIMA commercial software version 11.0 (EDILCLIMA 2021), which performs static and dynamic energy calculations that conform with Italian building energy performance legislation. In this study, the energy demand for space heating and cooling of buildings was determined through steady-state energy simulations for the duration of specific heating and cooling seasons, which are specified by local Italian design standards (UNI 2016). The steady-state assessment method was chosen for the assessment procedure over the more detailed dynamic simulation method because it is the method adopted by Italian design codes for the assessment and energy classification of local building stock (UNI 2014a). For energy assessments in parts of the world outside of Italy, other software tools such as EnergyPlus (2022) can be used.

The ERMs were designed to meet the performance requirements described in the Italian Ministerial Decree (Il Ministro Dello Sviluppo Economico 2015), which stipulates three different combinations of performance criteria that must be met depending on the severity of the intervention methods. For small-scale interventions, these criteria generally consist of, for example, ensuring that the thermal transmissivity of the retrofitted components is lower than a code-defined value. For large-scale interventions, the performance of a retrofitted structure is assessed relative to the performance of a building of the same geometry and occupancy type but with code-defined thermal properties. The primary results obtained from this type of energy performance assessment were annual electricity and fossil fuel consumption. These were then converted into economic and environmental variables to be used in the MCDM phase of the evaluation procedure. The primary energy performance index (PEC), which represents the total energy consumption of a building in kWh/m^2, was also obtained. The PEC was used to determine a building's energy class rating, which is a system used in Italy to categorize the energy performance of buildings across a range of occupational classes and climate demands. The energy classes represent the performance of a building relative to a building with the same geometry and occupational class but with code-defined minimum thermal properties. The classes are represented by a 10-letter scale from A4–G; A4 represents high energy performance above the code minimum level, A1 the code minimum performance, and G poor energy performance. PEC and the rating class are useful metrics for comparing how effective different energy retrofit schemes are at improving a building's energy performance.

Table 3. Decision variables adopted for the selection of the optimal retrofit alternative

Group	Symbol	Description
Economic	C_1	Installation costs of the retrofit alternative
	C_2	Expected annual costs of the retrofitted structure
Environmental	C_3	Expected life-cycle environmental impacts of the retrofitted structure
Social	C_4	Annual probability of failure
	C_5	Duration of work/disruption to occupants
	C_6	Architectural impact
Technical	C_7	Need for specialized labor/technical design knowledge
	C_8	Required intervention at the foundation level

In this study, three different combinations of ERMs were considered, representing different levels of intervention severity. A summary of the ERMs adopted for each energy retrofit scheme are presented in Table 2. Envelope ERMs (column two of Table 2) aim to reduce heat energy lost to the external environment. Plant and services ERMs (column three of Table 3) increase the energy efficiency of systems operating within a building. A detailed description of the retrofit interventions is provided in the following sections.

Decision Assessment

In the decision assessment phase of the procedure, the outcomes of the seismic and energy retrofit assessment phases were combined to create the set of complete seismic and energy retrofit alternatives that an optimal solution could be selected from. The MCDM framework was adopted to facilitate the selection of the optimal combination of SRMs and ERMs. The methodology has been described extensively in works by Caterino et al. (2008) and Carofilis et al. (2022), but at its core, it provides a rational framework for considering the performance of different retrofit alternatives across a broad range of DVs and uses a weighted average method to select the optimal solution.

When following this procedure, a decision maker first selects a set of variables with which to evaluate the performance of each

design alternative. Subsequently, each variable is assigned a weight representing how important it is to the decision maker; a larger weight value indicates that a variable is considered more important to a decision maker than a variable with a smaller weight. Weights can be determined simply by the intuition of the decision maker, or they can be determined using more rigorous methods, such as the analytical hierarchy procedure (AHP) (Saaty 1980), for example. Third, a decision matrix that contains the values of each decision variable for each design alternative is developed. The values of the decision matrix are then normalized, and the ideal and least ideal solutions for each decision variable are determined (i.e., the best and worst performing design alternatives for each particular decision variable). Each design alternative is then compared to the ideal and least deal alternatives for each variable by calculating the *n*-space Euclidean distance between the decision matrix values for a design alternative and the ideal and least ideal alternatives. Last, the relative closeness of each alternative to the least ideal solution is calculated, and the alternative with the highest relative closeness (i.e., the alternative that is the farthest from the least ideal) is chosen as the preferred solution.

The DVs used in this study are presented in Table 3 and were based on those adopted in previous optimal retrofitting studies that used the MCDM framework (Caterino et al. 2008; Gentile and Galasso 2019), where the rationale for selecting DVs C_1, C_4, C_5, C_6, and C_7 can be found. For the remaining DVs, the expected annual cost of the retrofitted structure, C_2—which includes the maintenance of structural and energy retrofit interventions, annual energy costs (AEC), and the expected annual loss from seismic damage—was considered as it provides insight into the expected life-cycle costs of each alternative. C_4, the APF, which is characterized by the annual rate of structural damage that could cause collapse, was included in the assessment as a measure of structural safety and the ability of a structure to prevent loss of life during an earthquake event. The life-cycle environmental impacts (LCEI), C_3, was chosen as the representative environmental impact (EI) DV because it is a comprehensive parameter that encompasses all sources of environmental impact over the life of a structure (Caruso et al. 2020; Passoni et al. 2021).

In the present study, the four seismic and three energy retrofit schemes outlined in the preceeding sections, were combined, leading to 12 possible retrofit alternatives. Henceforth, the combined alternatives will be referred to using the notation $A_{S,E}$, where S and E are numbers indicating the seismic and energy retrofit schemes, respectively, that comprise the combined alternative. Once combined, the retrofit alternatives were evaluated to determine the values of each of the DVs indicated in Table 3. The weight vector used in this study to define the relative importance of the different DVs under consideration was determined using the AHP described by Caterino et al. (2008).

Application to Case-Study Structure

Description of Structure

The building chosen as the case study for this research was an RC MRF school building with URM infills located in Isola del Gran Sasso d'Italia, Abruzzo, Italy (Prota et al. 2020). The school consists of two aboveground stories and a small partial basement at the east end. The first and second floors each have an area of approximately 630 m^2 and interstory heights of 3.75 and 4.25 m, respectively. The structural system consists of two-way RC MRFs in the longitudinal and transverse directions. URM infills and partitions are present throughout the building, and large penetrations in the exterior infill allow for the presence of windows. Because this structure was built between the 1960s and 1970s, it is an example of typical Italian construction prior to the introduction of modern seismic design codes (Prota et al. 2020). A more detailed description of the building, along with architectural plans and elevations, can be found in Prota et al. (2020).

To investigate how the choice of an optimal retrofit alternative is affected by different combinations of climatic conditions and seismic hazards, the case-study structure was assumed to be located in three different locations in Italy, all of which experience similar moderate to high levels of seismicity but have cold (C), moderate (M), and warm (W) climates. Città di Castello (latitude 43.4700° N, longitude 12.2314° E) was assumed to be representative of a C-type site, and Isola del Gran Sasso d'Italia (latitude 42.5056° N, longitude 13.6592° E) and Catania (latitude 37.5013° N, longitude 15.0742° E) were considered representative of M-type and W-type sites, respectively. Each of the sites is indicated in Fig. 1, which depicts climate conditions in terms of heating degree days (HDD) and seismic demands across Italy in terms of peak ground acceleration (PGA) on rock at the 712-year return period (life-safety return period for building class III according to NTC 2018).

Seismic Performance Assessment

Modeling and Preliminary Assessment

A numerical model of the case-study building was developed using the OpenSees version 3.3.0 software framework (McKenna et al. 2010), and a three-dimensional representation of the model is presented in Fig. 2. The model consists of flexural elements (i.e., beams and columns), beam-column joints (BCJs), a staircase, and masonry infill. Typical frame elements (beams, columns, and BCJs) were modeled following the suggestions presented by O'Reilly and Sullivan (2019) for simulating the structural behavior of older Italian RC frames. The staircases were modeled using simple elastic frame elements, with one element representing each stair unit. Concrete and steel material properties were obtained from Prota et al. (2020). More information on the modeling of the RC frame elements for this case-study structure can be found in the studies of Carofilis et al. (2020, 2021). Equivalent diagonal struts were used to model the effects of the URM infill; details were elaborated in previous studies by the authors (Clemett et al. 2022). In addition to the modeling of specific structural elements, the *laterizio* floor system was assumed to be rigid; as is typical in other similar studies (Caruso et al. 2020; Gabbianelli et al. 2020; O'Reilly et al. 2018). Second-order geometric effects were modeled using the P-Δ formulation. The base nodes of the numerical model were considered fully fixed, and any effects resulting from soil–structure interactions were neglected. Last, 5% tangent stiffness proportional Rayleigh damping was adopted at the frequencies of the first and third fundamental modes of vibration.

As previously mentioned, it was assumed that the ERMs do not affect the structural response of retrofitted buildings. This can be justified by the fact that the majority of energy retrofit measures apply to nonstructural components, such as windows or lighting systems, or to the slab elements, such as the roof and ground floor, all of which are not typically included in structural analyses. With regard to the addition of insulation panels to the masonry infills—it is conceivable that these could have an effect on the lateral strength and stiffness of the infill; however, because the infills were separated from the frame as part of the seismic retrofit schemes, this is unlikely to affect the global response of the structure.

The results of the preliminary seismic assessment are presented, for each site (C, M, W), in Figs. 3 and 4 as pushover curves indicating the four limit-state demands defined in NTC [immediate

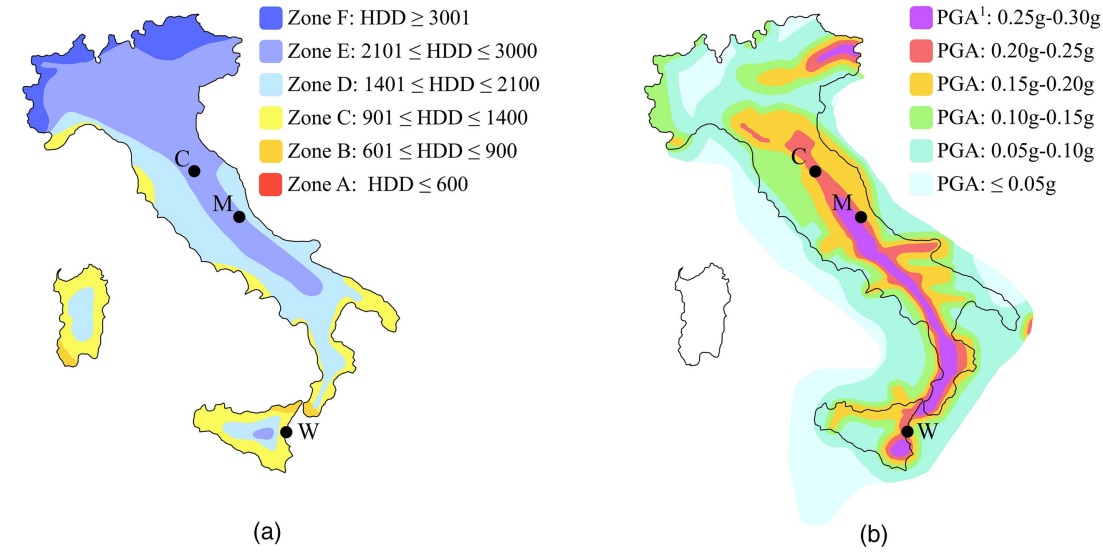

Fig. 1. (a) Climate conditions; and (b) seismic hazard at each of the sites (C, M, and W) investigated in this study. [Reprinted from Menna et al. 2019, under Creative Commons-BY-3.0 license (https://creativecommons.org/licenses/by/3/0/).]

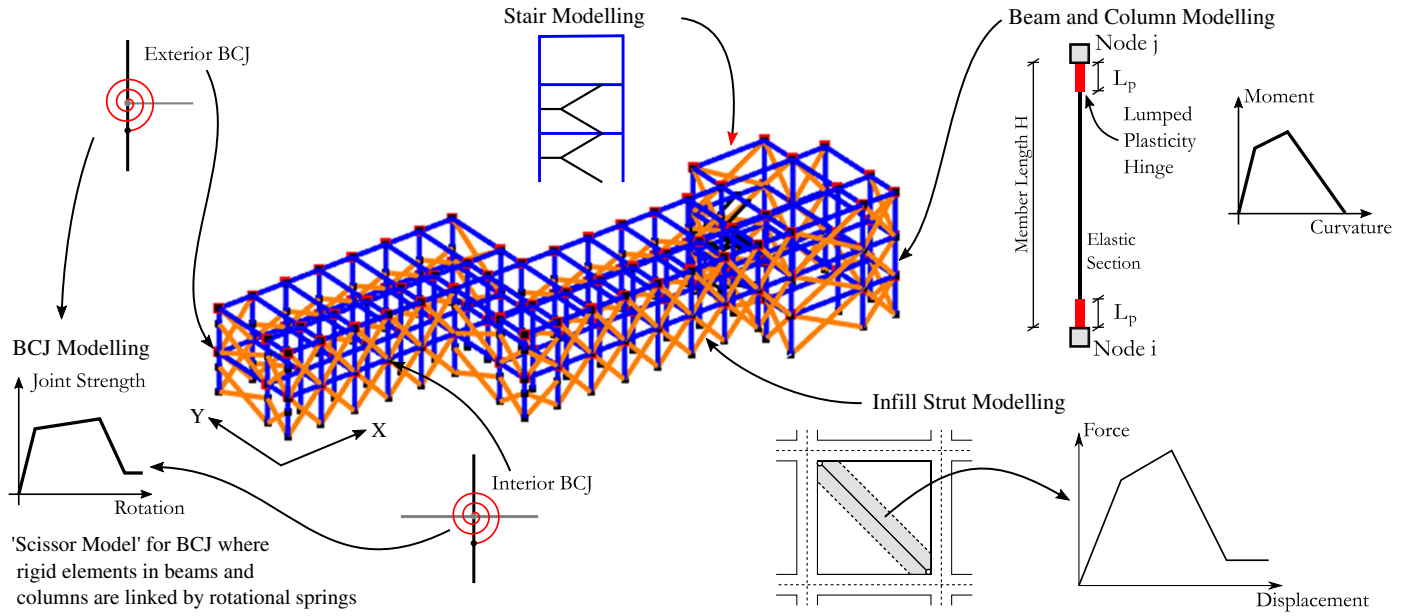

Fig. 2. Three-dimensional representation of the numerical model developed in OpenSees. (Adapted from *Engineering Structures*, Vol. 225, W. Carofilis, D. Perrone, G. J. O'Reilly, R. Monteiro, and A. Filiatrault, "Seismic retrofit of existing school buildings in Italy: Performance evaluation and loss estimation," 111243, © 2020, with permission from Elsevier.)

occupancy (SLO), damage limitation (SLD), life safety (SLV), and near collapse (SLC)], the limit-state capacities of the structure, and the corresponding drift profiles. The higher base shear coefficients observed in the *y*-direction can be attributed to the fact that the columns are bending about their major axis (Prota et al. 2020).

The preliminary assessment identified the moment capacity of the BCJs at which tensile cracking occurs and the shear capacity of the short columns adjacent to the URM infills as the critical structural weaknesses. These elements limit the performance of the structure to such an extent that the expected lateral capacity of the structure is between 13% and 15% of the anticipated demand at the SLV limit state.

Preliminary Assessment of the Seismic Retrofit Schemes

To address the critical structural weaknesses identified in the previous section, the four structural retrofit schemes introduced previously were designed and applied to the case-study structure. Additional considerations for modeling the retrofitted structures in OpenSees are described in Carofilis Gallo et al. (2021) and Clemett et al. (2022).

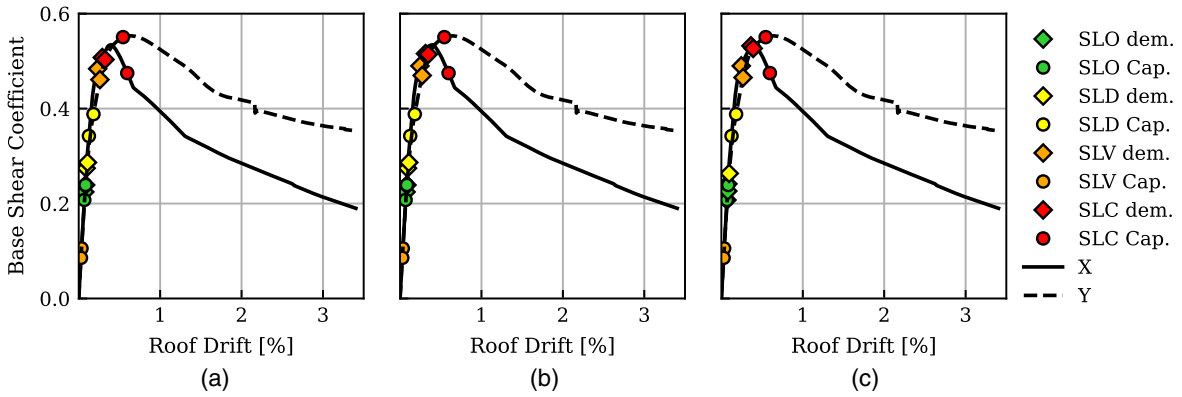

Fig. 3. Pushover curves showing the N2 performance points (diamonds) and the capacity (circles) at each limit state for the as-built structure: (a) Site C; (b) Site M; and (c) Site W.

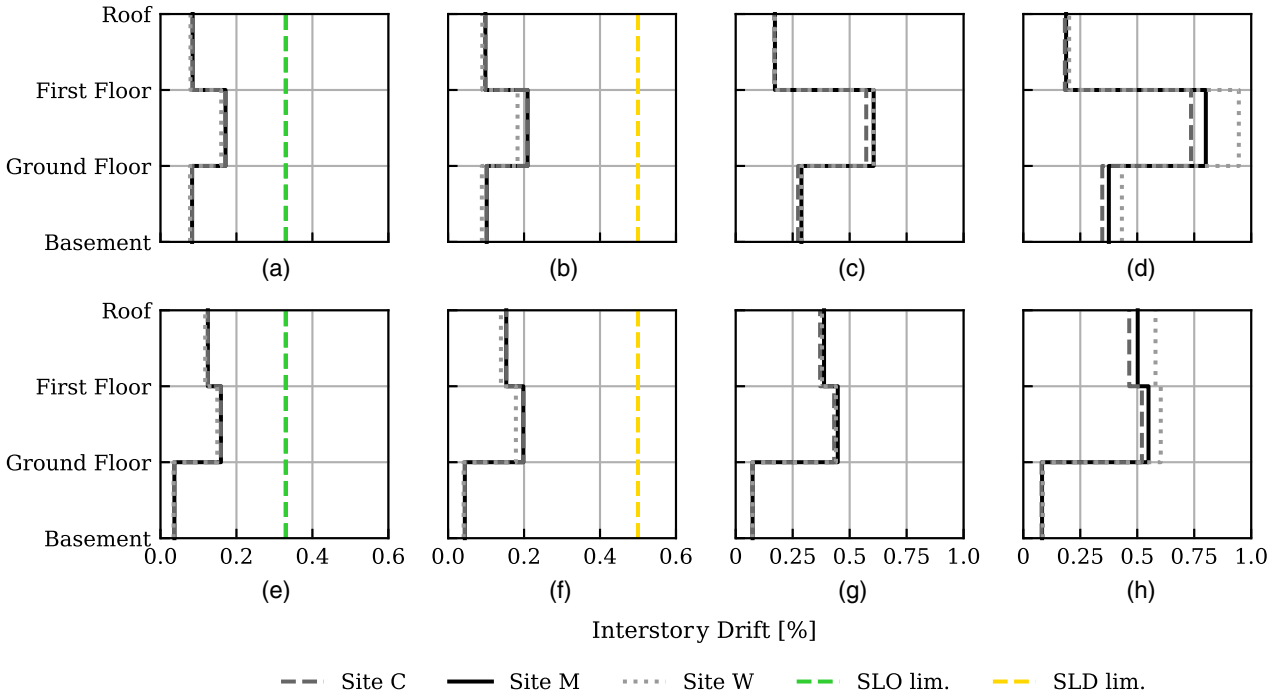

Fig. 4. Drift profiles of the as-built structure for the SLO, SLD, SLV, and SLC limit states in the (a–d) *x*-direction; and (e–h) *y*-direction.

The preliminary seismic assessment of the structural retrofit schemes was conducted using the same N2 method used for assessing as-built structure. The results of these assessments for Site C are presented in Figs. 5 and 6, which present pushover curves with limit state demands and capacities and limit state drifts, respectively. For brevity, the results for Site M and Site W are not presented, given that, due to the similar seismicity at each of the sites, few differences were observed in the response of the buildings.

In all cases, the structural retrofit schemes resulted in an improvement in the base shear capacity of the structure at the life safety limit state, which is, in general, greater than 45% of the level required for new code-compliant buildings. S3 and S4 exhibited the largest improvements in base shear capacity at each of the three sites, achieving capacities between 75% and 102% of the code-specified demand. S1 exhibited the lowest improvement of all the retrofit schemes, achieving base shear capacities between 37% and 45% in the *x*-direction and 45%–55% in the *y*-direction. It is worth noting that the total base shear capacity of S1 increased significantly and was higher than both S2 and S4; however, the increased strength and reduced ductility of the structure resulted in a much higher base-shear demand.

The interstory drifts were larger for the retrofitted alternatives than they were for the as-built structure; this was a direct result of the separation of the URM infill from the MRF. However, the drift profiles in Fig. 6 show that each of the retrofit schemes satisfied the code-specified limits.

Performance-Based Seismic Assessment

The second phase of the structural analysis was a comprehensive performance-based seismic assessment and loss analysis. The procedure that was followed and the assumptions that were made are detailed in Clemett et al. (2022). First, the seismic hazard at each of the three investigated sites was characterized, and a set of representative ground motions for each site were selected for use in the NLTHAs. The record sets were selected using the average spectral acceleration (AvgSA)–based selection procedure outlined

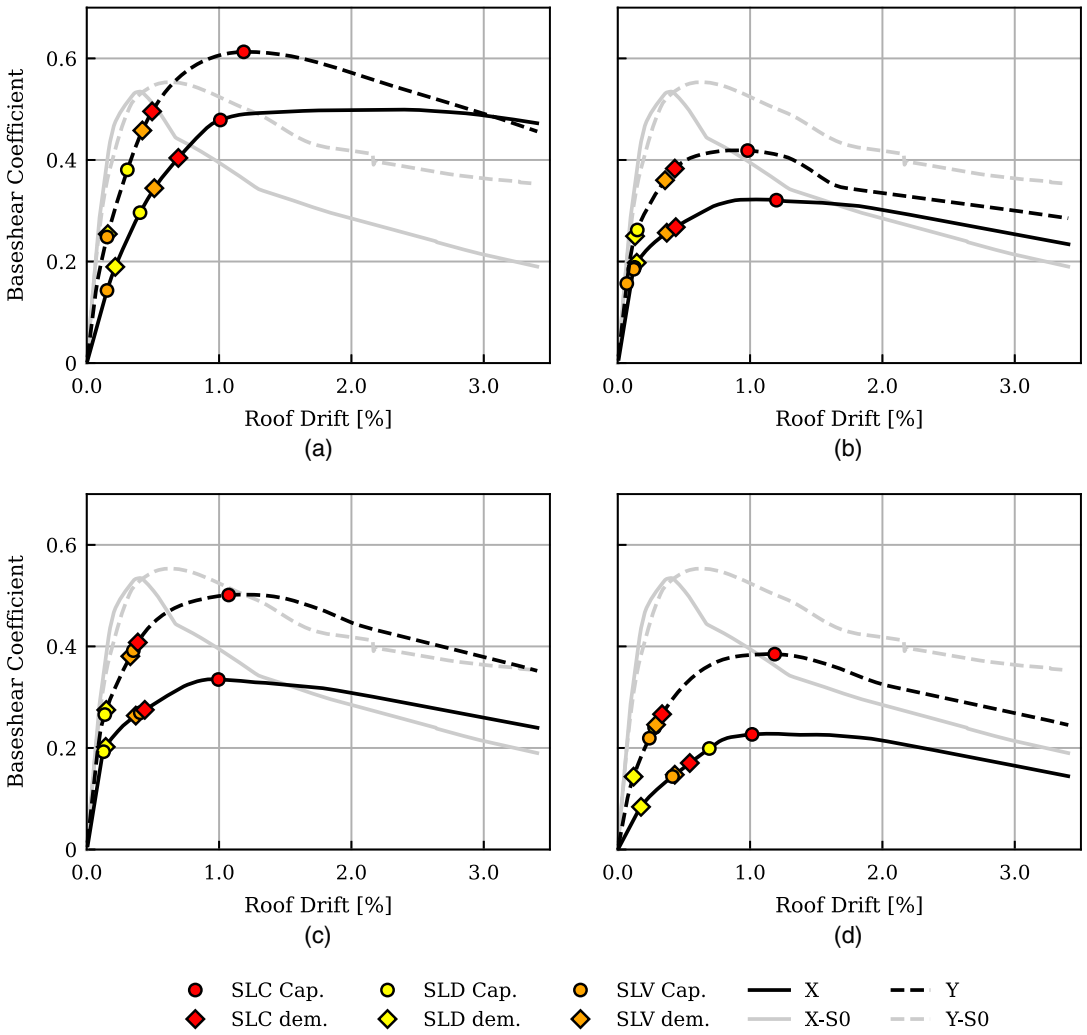

Fig. 5. Pushover curves and limit state demands and capacities for each of the retrofit schemes designed for Site C: (a) S1; (b) S2; (c) S3; and (d) S4.

in Carofilis Gallo et al. (2021). Second, using the record sets, a multiple-stripe analysis (MSA) was conducted for each of the sites. The key engineering demand parameters (EDPs) that were monitored and recorded for use in the loss assessment phase were absolute peak floor acceleration (PFA), peak story drift (PSD), and peak floor velocity (PFV). The nondirectional maximum of the medians of the maximum values observed for each EDP across all stories at each intensity in each direction are presented in Fig. 7. For brevity, only the MSA results from Site C are presented in Fig. 7, because there were no significant differences between the values obtained for the different sites. It is clear from Fig. 7 that S4, the retrofit scheme combining CFRP and dampers, provided a significant reduction in both PFA and PSD compared to the other alternatives. The drifts observed with retrofit schemes S1–S3 were larger than those of the as-built structure, and the accelerations were lower. This can be attributed to a reduction in the stiffness of the building caused by the separation of the concrete frame and masonry infill. Above a return period of approximately 700 years, a large increase in the PSD was observed, which can be attributed to the beginning of the formation of the plastic mechanism within the structure, which eventually leads to collapse at the highest intensity levels.

In addition, the collapse fragility parameters were determined from the MSA results. The median AvgSA and dispersion (β) values were modified to account for additional modeling uncertainty (O'Reilly and Sullivan 2018), and the final values used in the loss assessment are presented in Table 4. The collapse fragility curve for the as-built structure (S0) was included for comparison.

Third, an inventory of damageable components in the building, their potential damage states, and expected repair costs and EI consequences was developed. It was at this stage that the combination of the seismic and energy retrofit schemes had to be considered, because, as previous studies have highlighted, the value of ERMs can significantly influence the results of the loss assessment (Calvi et al. 2016; Mauro et al. 2017; Menna et al. 2019). This study utilized the component inventory that was developed as part of recent work by Clemett et al. (2022); it was modified to account for additional repair consequences associated with the different ERMs. These changes are summarized in Table 5 and are consistent with the approach used in previous studies (Mauro et al. 2017).

The final step in the detailed seismic assessment was the loss analysis. In addition to the inventory of damageable components, an estimate of replacement costs and replacement environmental impacts was required. This study assumed a basic replacement cost of €2,652, 242 and replacement EI of 1,830,000 kgCO_2e (Clemett et al. 2022) for the as-built structure. To account for increased building value associated with the different energy retrofit schemes, the replacement costs and EIs were increased in proportion to the

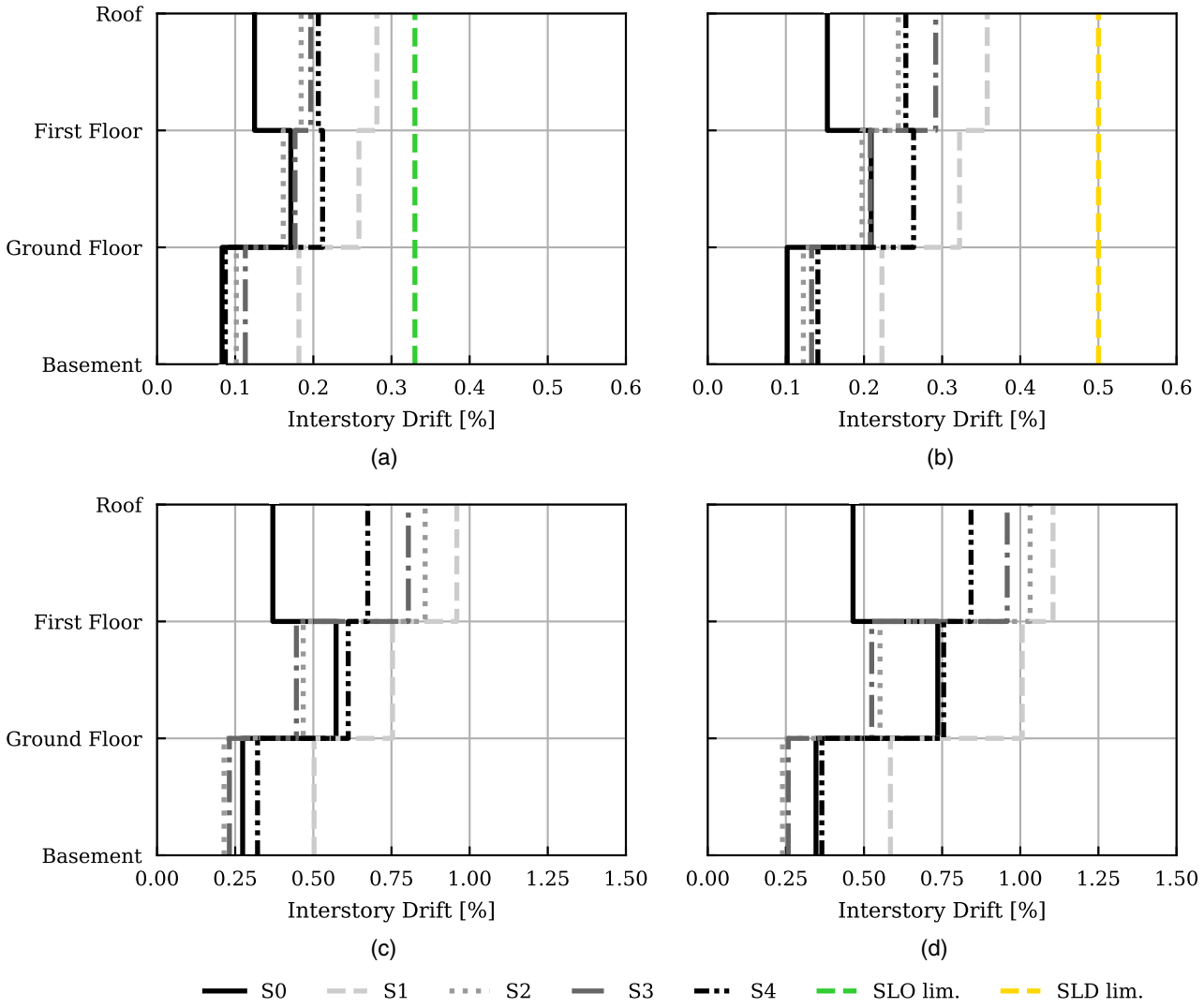

Fig. 6. Limit state drifts for each of the retrofit schemes designed for Site C: (a) SLO; (b) SLD; (c) SLV; and (d) SLC.

expected material costs of the ERMs, following the environmental economic input-output life cycle assessment (EEIOLCA) procedure described by Clemett et al. (2022). The replacement costs and EIs used in the loss assessment for the different retrofit combinations are shown in Table 6, in which S_i indicates that the replacement values depend only on the energy retrofit scheme and are independent of the structural retrofit scheme employed. For simplicity, it was assumed that only the ERMs, as opposed to the SRMs, increase the value of the building above the cost of the as-built configuration.

Using the data summarized in the foregoing, a detailed loss assessment of the 12 retrofit alternatives at each of the three sites was performed. The EAL, EAEI, and APF for each retrofit combination are presented in Table 7. The results for the as-built structure are also presented (A_{00}).

Energy Performance Assessment

Modeling and Preliminary Assessment

The energy performance of the case-study building was assessed using the EDILCLIMA software (EDILCLIMA 2021). The monthly weather data used in this study to specify the thermal loads was obtained from UNI 10349:2016 (UNI 2016). The majority of the modeling parameters were defined by local design codes based on the building's occupancy class, which, for a school building, is E.7 (Italian Government 1993; UNI 2014a, b). The case-study building was modeled using four different thermal zones representing the basement, ground floor, first floor, and the stairwell. All thermal zones were considered conditioned, with heating and cooling setpoint temperatures of 20°C and 26°C, respectively. The internal heat gain of 4 W/m^2 recommended by UNI 11300-1 (UNI 2014a) accounts for the additional heat energy produced by building occupants. Additional internal heat gains due to the domestic hot water system and electrical and plant equipment were not explicitly considered. Ventilation of the building was assumed to be provided naturally (i.e., no mechanical ventilation plant), and the air exchange method was used to model its effect. A value of one complete air change per hour (1 vol/h) was adopted to represent the low airtightness of the building prior to retrofitting (Pohoryles et al. 2020). The lighting power demand was adopted from suggested values for different room typologies (Recommended Lighting Levels in Buildings 2021), and the expected operational time was obtained from UNI 11300-2 (UNI 2014b). In addition, emergency lighting and control devices were assumed to use a total of 6.0 kWh of electricity per year (UNI 2014b).

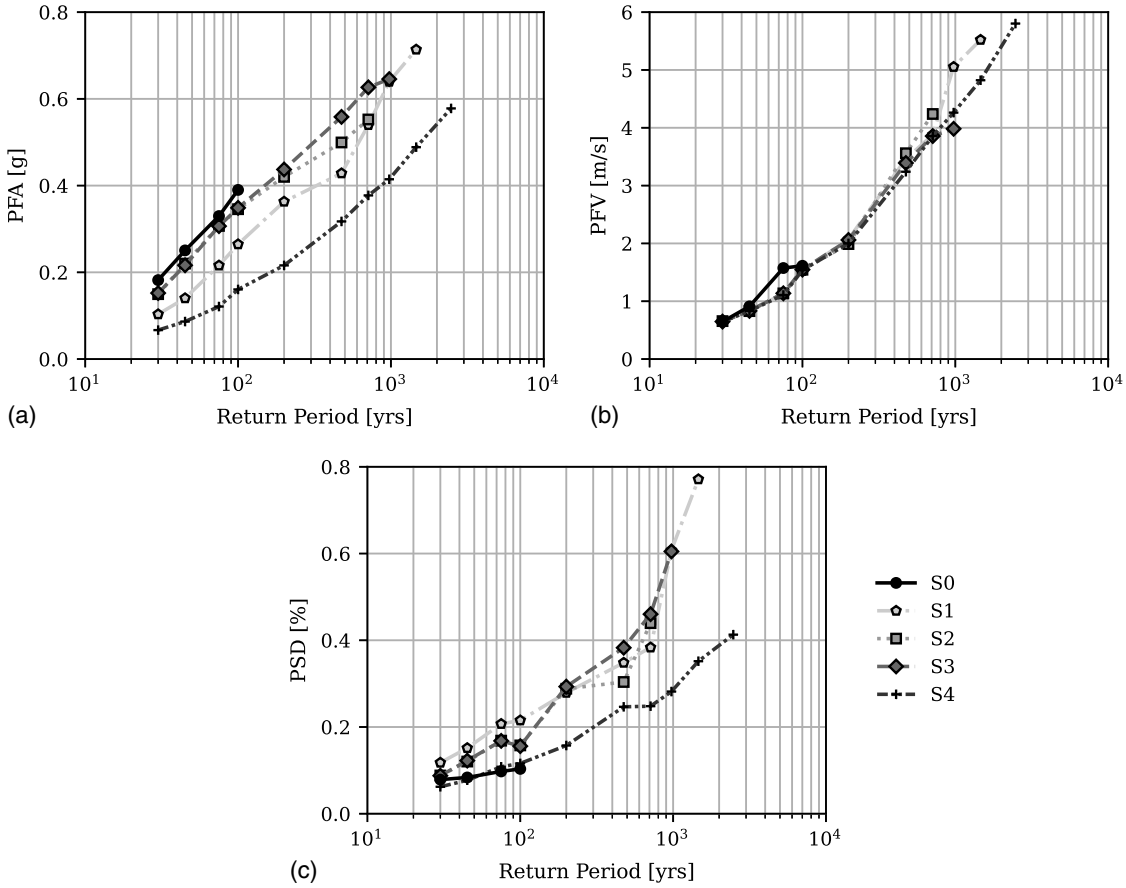

Fig. 7. Median nondirectional PFA, PFV, and PSD recorded at each intensity level during the MSA for Site C.

Table 4. Collapse fragility parameters of the structural retrofit schemes, modified to account for additional modeling uncertainties

	Site C		Site M		Site W	
Scheme	Median (g)	β	Median (g)	β	Median (g)	β
S0	0.107	0.401	0.118	0.400	0.116	0.420
S1	0.291	0.442	0.353	0.412	0.359	0.400
S2	0.225	0.464	0.238	0.445	0.238	0.435
S3	0.324	0.396	0.328	0.468	0.336	0.474
S4	0.565	0.426	0.537	0.409	0.522	0.348

The building envelope was modeled using centerline dimensions, and the thermal properties of the envelope elements were determined by defining the stratigraphy of each component's constituent materials. The total thermal transmissivities (U-values) of the envelope elements are summarized in Table 8. The values presented in the table include the thermal surface resistances and the slab-on-ground effect (when appropriate). Thermal bridges were included to correct for the two-dimensional heat flow that occurs at the intersections of different building elements. Thermal bridges were modeled at intersections between external wall elements;

Table 5. Influence of the ERMs on the consequences of repair in the damageable component inventory

Energy retrofit measure	Effect on loss assessment
Roof insulation with EPS panels	This ERM is applied to the roof, which, as a rigid diaphragm, is assumed to be undamaged. The cost is accounted for in the increased replacement cost of the structure.
Wall insulation with EPS panels	This ERM is applied to the existing walls, and the consequences are added to the existing fragility models. The cost is increased depending on the thickness of the insulation.
Floor insulation with EPS panels	This ERM is applied to the floor slab, which is assumed to be undamaged. The cost is accounted for in the increased replacement cost of the structure.
High performance windows	The replacement cost of the window components is increased depending on the type of window considered.
LED lighting	The value of the lighting units is increased to represent the increased cost of LED bulbs.
Lighting controls	The cost of lighting controls was not considered to affect the repair consequences of any existing components. The cost is accounted for by the increased replacement cost of the structure.
Thermostatic valves	The cost of this ERM is very low, and the added value to the repair consequences of the existing pipe components is negligible.
Condensing boiler	This ERM affects the value of the boiler. The replacement value was increased to represent the new equipment.
Photovoltaic panels	This ERM is applied to the roof, which, as a rigid diaphragm, is assumed to be undamaged. The cost is accounted for in the increased replacement cost of the structure.

Table 6. Replacement costs and EIs used in the loss analysis for the combined retrofit alternatives

	Site C		Site M		Site W	
Alt.	€	$kgCO_2e$	€	$kgCO_2e$	€	$kgCO_2e$
S_iE_1	2,703,835	1,869,777	2,700,684	1,867,485	2,688,077	1,858,315
S_iE_2	2,744,588	1,899,420	2,729,918	1,888,749	2,712,451	1,876,044
S_iE_3	2,890,738	2,005,724	2,858,340	1,982,159	2,841,825	1,970,146

Note: Alt. = Alternative.

external and internal wall elements; external walls and RC columns; external walls and roof/suspended floors/ground floors; and external walls and windows. The thermal transmissivity of the windows was adopted from UNI 11300-1 (UNI 2014a) assuming air filled double-glazed windows with metal frames and no low emissivity coatings. The nominal solar transmittance of the windows was assumed to be 0.750 (UNI 2014a). It was assumed that white internal curtains were present to help regulate the building's solar heat gains during the summer months. No external shading of the envelope from local topography or special shading devices was considered in the model.

Heating energy was assumed to be supplied by a traditional natural gas boiler system. A boiler efficiency of $\eta = 0.8$ was adopted to model the reduced performance of an aging heating system and was consistent with values adopted in other studies, such as Menna et al. (2021). In addition, distribution and control efficiencies were accounted for, assuming a poorly insulated horizontal distribution system and room temperature control provided by a single thermostat located at the boiler outlet. Distribution of the heated water was assumed to use 55 W of electricity. The heat from the water was imparted to the rooms through fan-coil heat exchangers, which are a common component of school buildings (Perrone et al. 2020). The nominal power of the emitters was assumed to be equal to the power of winter thermal losses through the building envelope. The nominal power of the emitters was assumed to be 60 W (UNI 2014b). Domestic hot water demand was assumed to be 0.2 L per person per day (UNI 2014b). The total number of building occupants was estimated from the office and seating layout of the school to be 235 people. This equated to a hot water demand of 47 L/day. Domestic hot water was assumed to be provided by the same heating system used for space heating.

The resulting PECs, equivalent CO_2 emissions, AECs, and Italian energy class ratings for the case-study building, located at each of the three study locations, are presented in Table 9. Electricity and natural gas consumption, which are direct outputs from the EDILCLIMA model, can be used to calculate equivalent CO_2 emissions and PEC using conversion factors calibrated to represent the characteristics of Italian electricity generation and natural gas production (Il Ministro Dello Sviluppo Economico 2015; UNI 2014c). AEC was calculated using the nonresidential electricity and natural gas pricing data for Italy in June 2020 (Eurostat—Electricity Prices 2021; Eurostat—Natural Gas Prices 2021), including taxes and levies. The electricity and natural gas costs adopted were 0.1753 €/kWh and 0.0291 €/kWh, respectively. Last, the energy class rating was determined by comparing the PEC of the case-study building to a code-defined reference building (Il Ministro Dello Sviluppo Economico 2015).

Modeling and Assessment of the Energy Retrofit Schemes

Three different energy retrofit schemes, were considered for each climate zone and designed in accordance with local legislative requirements. Each retrofit scheme was modeled in EDILCLIMA using the same basic parameters as the as-built structure. Additional modeling considerations for each retrofit intervention are summarized in the following paragraphs.

The EPS insulation panels used for the roof and walls were assumed to have a thermal conductivity of 0.035 W/mK (Building Envelope 2019). The thickness of the insulation was designed to ensure that the U-value of the retrofitted elements met the minimum code requirements (Il Ministro Dello Sviluppo Economico 2015). The final U-values and corresponding insulation thicknesses for each retrofit scheme are presented in Table 10. Floor insulation was provided as part of the E3 scheme for Site C to satisfy the more stringent code requirements for the average thermal transmissivity of the building envelope. A 20-mm layer of EPS insulation, with the same thermal properties as the roof and wall insulation, was applied directly to the slab-on-grade and overlaid with vinyl-rubber flooring. The thermal transmissivities of the new window elements were adopted from UNI 11300-1 (UNI 2014a), assuming six-chamber PVC frames and the glass properties summarized in Table 11. It was assumed that the original curtains were replaced with white internal venetian blinds in the classrooms and toilet areas to reduce solar heat gain during the summer. A curtain factor of 0.25 was adopted from UNI 11300-1 (UNI 2014a) to capture this effect. In addition to increased thermal resistance, the new windows were assumed to improve the airtightness of the structure. This improvement was modeled by reducing the number of air changes to 0.5 vol/h for the E3 retrofit scheme. The replacement of existing fluorescent tube lights with LED lights was modeled by assuming that the more efficient LEDs required 50% less

Table 7. EAL, EAEI, and APF obtained from the detailed loss assessment for each of the 12 alternatives for each location investigated

	Site C			Site M			Site W		
Alt.	EAL (€)	EAEI ($kgCO_2e$)	APF ($\times 10^{-2}$)	EAL (€)	EAEI ($kgCO_2e$)	APF ($\times 10^{-2}$)	EAL (€)	EAEI ($kgCO_2e$)	APF ($\times 10^{-2}$)
A_{00}	38,557	26,357	1.139	34,151	23,344	1.002	34,459	23,565	1.004
A_{11}	9,399	6,081	0.267	6,775	4,240	0.166	4,913	2,998	0.101
A_{12}	10,009	6,544	0.290	7,320	4,634	0.187	5,116	3,158	0.108
A_{13}	10,727	7,022	0.294	7,478	4,755	0.181	5,376	3,347	0.112
A_{21}	16,130	10,238	0.458	15,897	10,099	0.455	10,664	6,634	0.286
A_{22}	16,304	10,421	0.473	15,982	10,279	0.470	10,863	6,789	0.293
A_{23}	17,031	10,936	0.469	16,065	10,340	0.437	12,265	7,794	0.330
A_{31}	9,601	5,565	0.205	10,115	6,051	0.246	7,482	4,352	0.166
A_{32}	10,095	5,979	0.230	10,657	6,452	0.266	7,600	4,424	0.167
A_{33}	10,531	6,247	0.224	11,464	6,996	0.274	7,711	4,503	0.162
A_{41}	3,083	1,745	0.052	3,452	2,045	0.079	2,512	1,427	0.043
A_{42}	3,213	1,846	0.057	3,585	2,138	0.074	2,579	1,477	0.040
A_{43}	3,321	1,913	0.054	3,593	2,134	0.068	3,302	1,943	0.059

Note: Alt. = Alternative. All costs are expressed in euros in June 2020.

Table 8. Thermal transmissivities of the external envelope components excluding thermal bridge effects

Envelope element	U-value (W/m^2 K)
External walls	0.809
External basement walls	0.388
Ground floor slab-on-grade	0.541
Basement floor slab-on-grade	0.435
Roof	1.609
Windows	4.1

Table 9. Performance summary of the case-study building in the as-built configuration at each site

Parameter	Units	Site C	Site M	Site W
PEC	kWh/m^2	372	309	164
Eq. CO_2	$kgCO_2e$	92,192	76,651	40,337
Annual energy cost	€ (June 2020)	14,878	12,718	7,646
Energy class	—	F	E	D

Table 10. U-values of the retrofitted wall and roof elements, excluding thermal bridge effects

		U-values in W/m^2 K [insulation thickness (mm)]	
Site	Scheme	Roof	Wall
C	E1	0.202 (150)	—
	E2	0.202 (150)	0.182 (150)
	E3	0.202 (150)	0.182 (150)
M	E1	0.215 (140)	—
	E2	0.215 (140)	0.230 (110)
	E3	0.215 (140)	0.213 (120)
W	E1	0.285 (100)	—
	E2	0.285 (100)	0.287 (80)
	E3	0.245 (120)	0.247 (100)

Note: In columns 3 and 4, insulation thickness (in mm) is indicated in parentheses.

electricity to produce the same level of illumination in each room (metroLED 2014). The installation of thermostatic valves was modeled by increasing room temperature regulation efficiency, as detailed in the Italian design code (UNI 2014b). The thermostatic valves were assumed to have a proportional band of 1°C. The new condensing boiler was assumed to have a nominal combustion power of 60 kW and a nominal efficiency of $\eta = 1.07$. The new lighting control system employed required manual switching on of lights with automatic switching off when a room was unoccupied. An appropriate control reduction factor (0.80) was obtained from UNI EN 15193 (UNI 2008). Last, 20 160-W polycrystalline photovoltaic panels, oriented to the south, were installed on the roof of the school as part of the E3 retrofit scheme.

The results of the energy performance assessment are presented in Table 12. The AECs and the energy class ratings indicate that all the retrofit schemes successfully improved the energy performance of the structure at each of the sites investigated. The first level of retrofit (E1) resulted in a 28%–35% reduction in annual PEC. Similar trends were seen in the results of the E2 and E3 retrofit schemes, which exhibited reductions in the range of 46%–50% and 75%–80%, respectively. At all three sites, the E3 retrofit scheme ensured equal or better performance than code minimum standard, with energy class ratings of A1 and A2 observed.

Decision Assessment

Determination of the Decision Matrix Values and Weight Vectors

This section details the methods that were used and the assumptions that were made to calculate the values of the decision variables and the weight vector for each of the decision assessments. The final decision variable values and the weight vectors are presented at the end of the section.

C1—Installation Cost: Installation cost is the combined cost of the seismic and energy retrofit schemes for each alternative, considering efficiencies that can be gained by implementing both retrofitting schemes simultaneously—for example, only accounting once for the hire of scaffolding, and so forth. The cost estimation of the seismic retrofit schemes has been described in previous work by the authors (Clemett et al. 2022); for the energy retrofits, the cost of the EPS insulation was estimated using data provided by Formisano et al. (2019). The costs of the condensing boiler unit and solar panels were obtained from the work of Mauro et al. (2017). The work of Sassun et al. (2016) was used to estimate the cost of alterations to existing blockwork and the plastering and finishing of the walls. The cost of the window units was estimated using cost estimate data available from the United States (Homewyse 2021). The cost data was converted from US dollars to Italian euros (in June 2020) using the methodology proposed by Silva et al. (2020). Cost premiums of 7.5% and 30% were assumed for the argon-filled double- and triple-glazed windows, respectively, over the standard air-filled double-glazed windows. An estimation of the cost of small retrofit items, such as LED tube lights and thermostatic valves, was obtained from data available on commercial retail websites. These assumptions and the final cost estimates were verified as reasonable values by a local energy retrofitting consultant in Pavia, Italy.

C2—Expected Annual Costs: The expected annual cost of a retrofit alternative comprises three parts; the EAL, the maintenance cost of the retrofit components, and the AEC. The EAL and the AEC were determined from the seismic and energy performance analyses, and the corresponding results can be found in Tables 7 and 12, respectively. The cost of structural maintenance over the lifetime of the structure (75 years) was obtained by considering the interventions outlined by Caterino et al. (2008) and scaling them based on the quantity of materials used. An annual inflation rate of 1% per year was used to calculate the increased costs associated with the various

Table 11. Window types adopted for the E3 retrofit scheme at each site and their corresponding thermal properties

Window property	Site C	Site M	Site W
Description	Argon-filled triple glazing, 4-8-4-8-4 glass, two panes with low emissivity (0.05) coatings	Argon-filled double glazing, 4-16-4 glass, one pane with low emissivity (0.05) coating	Air-filled double glazing, 4-12-4 glass, no coating
U-value (W/m^2 K)	1.2	1.4	2.6
Solar transmittance	0.500	0.670	0.750

Table 12. Performance summary of the retrofitted case-study building

Site	Scheme	PEC (kWh/m^2)	Eq. CO_2 ($kgCO_2e$)	AEC [€ (June 2020)]	Energy class
C	E1	257.48	63,872	10,355	D
	E2	199.41	48,564	8,218	D
	E3	73.22	16,919	3,445	A1
M	E1	221.76	52,476	8,765	D
	E2	166.63	40,716	7,121	C
	E3	64.92	14,982	3,109	A2
W	E1	106.4	26,118	51,012	C
	E2	81.5	19,822	4,210	B
	E3	40.34	8,828	2,198	A2

maintenance interventions in the future. The discounting of future costs to account for the benefits of investing money earmarked for future spending was not accounted for in this study, because it requires knowledge of capital assets and the income of the decision maker, which fall outside the scope of this study. However, these items are worth considering on a project-specific basis. Concerning the energy retrofit, it was assumed that the EPS insulation would not require any maintenance; however, visual inspection of the plaster finish would be required every 5 years, with minor patching required to ensure weather tightness. The cost of the visual inspection was assumed equal to the cost of concrete visual inspections reported by Caterino et al. (2008). Complete replacement of the LED lights was assumed to be required every 16 years. The maintenance of the solar panel was assumed to comprise biannual cleaning of the panels, an annual professional inspection, and one panel replacement every 10 years to account for potential damage. To calculate the expected annual costs, the EAL and AEC were multiplied by the nominal design life of the building and added to the total maintenance costs. This value was then normalized by the nominal life of the structure and the floor area in a procedure analogous to the life-cycle performance metric proposed by Caruso et al. (2020).

C3—Expected LCEI: The expected LCEI value was calculated using Eq. (1) (Caruso et al. 2020):

$$\text{LCEI} = \frac{\text{IEI} + \text{EAEI}_{\text{postretrofit}} \times \text{SL} + \text{MEI}}{A \times \text{SL}} \tag{1}$$

where IEI = installation EI of the retrofit alternative; $\text{EAEI}_{\text{postretrofit}}$ = EAEI of the retrofitted structure; SL = expected service life of the structure postretrofit; MEI = total maintenance EI of the alternative over the expected service life; and A = total floor area of the building. The value of each component was determined following the procedure described in previous work by the authors (Clemett et al. 2022).

C4—Annual probability of failure: The values for the annual probability of collapse were determined from the results of the detailed seismic performance assessment (i.e., using PACT) and can be found in Table 7.

C5—Duration of works: The data presented by Mazzolani et al. (2018) and found on Homewyse (2021) were used to estimate the duration of the structural intervention works. The reference values were scaled based on material quantities and floor area when appropriate, and it was assumed that a maximum of 60 workers were present on site at a given time. The contribution of the energy retrofitting schemes to the overall duration of work was accounted for by adding a fixed number of days (assuming an additional 20 workers) to the duration estimates of the structural interventions. These assumptions are detailed in Table 13.

Table 13. Assumptions for the additional contributions of the energy retrofit schemes (in days) to the total duration of work for the combined alternatives

Structural retrofit scheme	Energy retrofit scheme		
	E_1	E_2	E_3
$S_1/S_3/S_4$	3	3	7
S_2	3	5	10

C6—Architectural Impact: A qualitative ranking of the alternatives based on their architectural impact was performed using AHP, as described by Caterino et al. (2008). The preference matrix used in this study was based on the professional judgment of the authors. This matrix only considered the impact of the structural retrofit schemes, because the energy retrofit schemes were all assumed to have a similarly low visual impact once construction was complete.

C7—Need for specialized labor/design knowledge: The values for this variable were determined using AHP and the judgment of the authors in a procedure analogous to the one used in C_5.

C8—Required interventions at the foundations: The maximum ratio of the vertical support reactions between the as-built case-study building and each of the retrofit alternatives was used to represent the amount of work required to improve the foundations of the existing structure to cope with the loads of the retrofitted structure.

Weight Vector: The weight vector, one of many possible acceptable vectors, was determined using AHP and the professional judgment of the authors. The following assumptions guided the selection of the values for the pairwise comparisons of the variables: (1) the decision maker was assumed to be the owner and operator of the building—this is not unreasonable, because the state generally provides funding for capital and ongoing expenditures of school buildings—therefore, C_1 and C_2 were almost equal, with slight preference given to ongoing costs; (2) sustainability is a key consideration in modern designs—C_3 (EIs) was considered to be equally as important as the cost variables; (3) the annual probability of failure, C_4, is a very relevant variable and was considered to be as important as the installation cost of the building and the LCEIs; (4) the retrofit interventions must be able to be completed during the summer holiday period when the school is empty—therefore, C_5 was considered to be almost as important as the cost-related variables; (5) a school building is relatively insensitive to architectural changes unless they directly impact the work space, which is an uncommon occurrence—therefore C_6 was given low importance relative to the other variables; (6) Italy is a seismically active country with many aging buildings requiring retrofit; (7) assuming that most engineers and contractors are familiar with common retrofit concepts and techniques, C_7, specialist design knowledge and installation skills, was considered less important in this study; and (8) C_8, intervention at the foundation, may represent an additional cost incurred during the installation of the retrofit alternatives; therefore this factor was given moderate importance. It is important to note that the choice of the weight vectors is the biggest source of uncertainty in the MCDM procedure, and it can significantly impact the results of the decision analysis (Carofilis et al. 2022).

The final values for the weight vectors and the decision variables are presented in Fig. 8 and Table 14, respectively.

Selection Results and Discussion

The decision matrices and weight vectors presented in the previous section were used as inputs to the MCDM procedure. The preferential rankings obtained from each analysis are presented in Fig. 9, in which the alternative in rank 1 is considered the most preferred

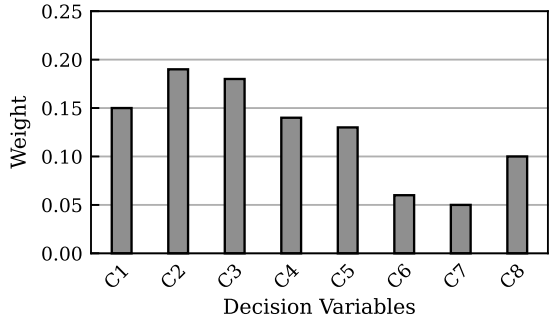

Fig. 8. Weight vectors used in the MCDM procedure.

option, given the selection criteria and weights, and the alternative in rank 12 is the least preferred. The values presented in the second column for each site indicate the relative closeness of each alternative to the fictitious ideal retrofit alternative, a parameter used to rank the alternatives in preferential order. The relative closeness values lie in the range (0,1), with a value of 1 indicating that an alternative is the ideal solution. The differences between the relative closeness values can be used to understand how strongly one solution is preferred over another. Shading has been used to easily identify differences in the rankings at each site. The different levels of shading correspond to the alternatives retrofitted with the different S1, S2, S3, and S4 retrofit schemes.

The results from Site W, where climate demands were less severe relative to seismic demand, exhibit a clear trend compared to the other sites. The rankings of the alternatives are grouped by structural retrofit scheme, with the S4 scheme being the most preferred option, followed by S3, S2, and finally S1. This trend indicates that, at least for the warmer site, the seismic retrofit scheme had a more significant effect on the overall ranking of an alternative than the energy retrofit scheme. Inspection of the relative closeness values indicates that the rankings of the first six alternatives were reasonably close, with only a 10% variation in the relative closeness between the alternatives ranked first and sixth; there was a more significant gap between the S3 and S2 alternatives. For a given structural retrofit scheme, it appears that, in general, the alternative with the E3 energy retrofit scheme is the least preferred alternative, and E2 is the most preferred. This tends to indicate that in warmer climates it may not be advantageous to provide maximum levels of energy efficiency retrofit (e.g., providing new roof and wall insulation and replacing the primary heating system), because the associated benefits do not outweigh the costs when considered in a combined seismic-energy MCDM framework. Further inspection of the relative closeness values across the three different energy retrofit schemes for a given

Table 14. Decision variable values for the selection of the optimal retrofit alternative

Site	Alt.	C_1 (€)	C_2 (€)	C_3 ($kgCO_2e$)	C_4 ($\times 10^{-2}$)	C_5 (days)	C_6	C_7	C_8
Site C	A_{11}	1,209,497	19.99	57.64	0.267	60	0.0227	0.0844	6.12
	A_{12}	1,293,366	19.36	47.69	0.290	60	0.0227	0.0844	6.12
	A_{13}	1,521,766	17.11	26.85	0.294	64	0.0227	0.0844	6.12
	A_{21}	190,167	20.79	54.83	0.458	22	0.0555	0.0135	16.49
	A_{22}	274,036	19.85	44.68	0.473	24	0.0555	0.0135	16.49
	A_{23}	502,435	17.61	23.87	0.469	29	0.0555	0.0135	16.49
	A_{31}	250,865	17.63	51.75	0.205	37	0.0934	0.0844	16.55
	A_{32}	334,734	16.92	41.77	0.230	37	0.0934	0.0844	16.55
	A_{33}	563,133	14.47	20.78	0.224	41	0.0934	0.0844	16.55
	A_{41}	609,778	17.92	50.10	0.052	44	0.1617	0.1511	5.14
	A_{42}	695,647	16.95	39.89	0.057	44	0.1617	0.1511	5.14
	A_{43}	922,046	14.26	18.75	0.054	48	0.1617	0.1511	5.14
Site M	A_{11}	1,229,555	16.87	48.28	0.166	61	0.0227	0.0844	5.71
	A_{12}	1,290,386	16.55	40.72	0.187	61	0.0227	0.0844	5.71
	A_{13}	1,462,370	14.45	23.49	0.181	65	0.0227	0.0844	5.71
	A_{21}	183,863	19.48	46.57	0.455	22	0.0555	0.0135	16.54
	A_{22}	244,694	18.83	38.83	0.470	24	0.0555	0.0135	16.54
	A_{23}	416,678	16.68	21.52	0.437	29	0.0555	0.0135	16.54
	A_{31}	297,092	18.07	44.19	0.246	42	0.0934	0.0844	16.61
	A_{32}	357,922	17.74	36.56	0.266	42	0.0934	0.0844	16.61
	A_{33}	529,907	16.10	19.67	0.274	46	0.0934	0.0844	16.61
	A_{41}	584,415	17.05	42.12	0.079	44	0.1617	0.1511	4.77
	A_{42}	645,245	16.43	34.27	0.074	44	0.1617	0.1511	4.77
	A_{43}	817,230	14.22	16.99	0.068	48	0.1617	0.1511	4.77
Site W	A_{11}	1,215,433	13.03	28.43	0.101	63	0.0227	0.0844	5.71
	A_{12}	1,266,544	13.00	24.58	0.108	63	0.0227	0.0844	5.71
	A_{13}	1,444,776	12.41	17.93	0.112	67	0.0227	0.0844	5.71
	A_{21}	158,651	13.11	25.04	0.286	22	0.0555	0.0135	16.54
	A_{22}	209,762	13.08	21.18	0.293	24	0.0555	0.0135	16.54
	A_{23}	387,993	13.30	15.12	0.330	29	0.0555	0.0135	16.54
	A_{31}	272,351	13.55	23.93	0.166	42	0.0934	0.0844	16.61
	A_{32}	323,462	13.46	20.01	0.167	42	0.0934	0.0844	16.61
	A_{33}	501,694	12.76	13.28	0.162	46	0.0934	0.0844	16.61
	A_{41}	532,024	13.66	22.62	0.043	43	0.1617	0.1511	4.80
	A_{42}	583,135	13.54	18.68	0.040	43	0.1617	0.1511	4.80
	A_{43}	761,367	13.27	12.23	0.059	47	0.1617	0.1511	4.80

Note: Alt. = Alternative.

Rank	Site C		Site M		Site W	
	Alternative	Rel. Clos.	Alternative	Rel. Clos.	Alternative	Rel. Clos.
1	A_{33}	0.6408	A_{43}	0.6325	A_{42}	0.6599
2	A_{43}	0.6182	A_{42}	0.617	A_{41}	0.6456
3	A_{32}	0.6098	A_{41}	0.5949	A_{43}	0.6326
4	A_{42}	0.6083	A_{33}	0.5924	A_{32}	0.6163
5	A_{31}	0.5903	A_{32}	0.5699	A_{33}	0.6143
6	A_{41}	0.584	A_{23}	0.5607	A_{31}	0.5996
7	A_{23}	0.5443	A_{31}	0.5577	A_{22}	0.5623
8	A_{22}	0.5239	A_{22}	0.5228	A_{21}	0.5585
9	A_{21}	0.5154	A_{21}	0.5168	A_{23}	0.5264
10	A_{13}	0.3987	A_{13}	0.4547	A_{12}	0.4426
11	A_{12}	0.3566	A_{11}	0.4198	A_{11}	0.4415
12	A_{11}	0.3553	A_{12}	0.4194	A_{13}	0.4385

Fig. 9. Rankings of the retrofit alternatives at each location obtained using the MCDM procedure.

structural retrofit scheme reveals that the variations of the relative closeness values are between 1% and 7%, depending on the structural scheme.

Looking at Site M, similar trends to those at Site W can be observed. Again, the ranking of alternatives is, generally, grouped according to the structural retrofit alternative, with the S4 alternatives preferred over the S3, S2, and S1 options. However, at this site, which has a much colder climate than Site W, the alternatives retrofitted with the E3 energy scheme are preferred over the E1 and E2 alternatives for each of the four structural retrofit schemes. The increasing importance of energy performance can be observed by the fact that, for this site, A23 is ranked higher than A33. This is a clear indication that the benefits of the improved E3 energy retrofit of A23 outweigh the better structural performance of A33, despite the higher installation costs associated with it. The variations in relative closeness values of alternatives with the same structural retrofit scheme but different energy retrofit schemes are between 3.5% and 8.5%.

The increasing influence of the energy retrofitting schemes is also evidenced in the rankings of the alternatives for Site C, which has the coldest climate of the three investigated sites. At this site, the top six ranking spots are still occupied by the S4 and S3 alternatives, although they alternate back and forth depending on the energy retrofit scheme adopted. The alternatives with the E3 scheme are the preferred choice, followed by E2 and E1. Despite this behavior, the overall variations of the top six alternatives remains around 10%. The variations of the relative closeness values for the alternatives with a given structural retrofit solution are between 4% and 8.5%, depending on the scheme.

Looking at the results across each of the sites, it appears that as heating demands increase, the impact of the energy retrofit alternatives on the ranking order becomes more important and, subsequently, the more energy-efficient retrofit alternatives are the preferred solutions. It is also interesting to note that the first-ranked alternative is different for each of the sites. This tends to indicate that for given sites with similar seismicity, climate demands affect the choice of the optimal combined retrofit alternative. Across all three sites, the S1 alternatives are consistently ranked as the least preferred alternatives, primarily due to their substantial installation costs, which are 2–6 times the cost of the other alternatives. The high installation costs are the result of requiring many CFRP bars, which are costly and labor intensive to install, to control structural drifts. This indicates that retrofit schemes using only CFRP to control global behavior are not efficient solutions, and superior results can be obtained using multiple intervention techniques, such as braces and CFRP or dampers and CFRP.

Conclusions

This paper presented a general and robust methodology for the selection of an optimal combination of seismic and energy retrofitting schemes from a set of predefined alternatives by utilizing an MCDM framework and investigated how the choice of an optimal solution varies for buildings located at sites with different combinations of seismic hazards and climate conditions. It was observed that climate demands have a significant impact on the choice of an optimal combined retrofit alternative. This is an important finding, particularly when considering a portfolio of buildings with a wide spatial distribution, such as school buildings owned by regional or national governing bodies, because it highlights that the same combination of energy and seismic retrofit may not be optimal in all locations. The difference between implementing optimal and nonoptimal solutions could prove significant; for example, if a decision maker is subject to strict environmental, social, or economic constraints. While this study was conducted with the intent of showcasing a decision-making framework that can be relatively easily implemented by design professionals, the detailed analysis methods used, particularly for seismic performance assessment, make the procedure somewhat time-consuming and computationally expensive. To make this methodology more attractive to practicing engineers, future research will focus on simplifying aspects of this procedure to make it more accessible and time-efficient. Such research developments possibly include investigating the use of simplified loss assessment techniques, such as the Italian seismic risk assessment guidelines (Sismabonus) or component-based loss assessment using the results from pushover analyses instead of complex time-history analyses, to see if they produce similar results to the detailed approach described herein.

Data Availability Statement

Some or all data, models, or code that support the findings of this study are available from the corresponding author upon reasonable request.

Acknowledgments

This work has been developed within the framework of the project "Dipartimenti di Eccellenza," funded by the Italian Ministry of Education, University, and Research, and ReLUIS 2019-2021, funded by the Italian Department of Civil Protection.

References

Asprone, D., F. Jalayer, S. Simonelli, A. Acconcia, A. Prota, and G. Manfredi. 2013. "Seismic insurance model for the Italian residential building stock." *Struct. Saf.* 44 (Sep): 70–79. https://doi.org/10.1016/j.strusafe.2013.06.001.

Building Envelope. 2019. *Handbook of energy efficiency in buildings*. Amsterdam, Netherlands: Elsevier.

Calvi, G. M. 2013. "Choices and criteria for seismic strengthening." *J. Earthquake Eng.* 17 (6): 769–802. https://doi.org/10.1080/13632469.2013.781556.

Calvi, G. M., L. Sousa, and C. Ruggeri. 2016. "Energy efficiency and seismic resilience: A common approach." In *Multi-hazard approaches to civil infrastructure engineering*, edited by P. Gardoni and J. M. LaFave, 165–208. Cham, Switzerland: Springer International Publishing.

Cardone, D., G. Gesualdi, and G. Perrone. 2019. "Cost-benefit analysis of alternative retrofit strategies for RC frame buildings." *J. Earthquake Eng.* 23 (2): 208–241. https://doi.org/10.1080/13632469.2017.1323041.

Carofilis, W., N. Clemett, G. Gabbianelli, G. O'Reilly, and R. Monteiro. 2022. "Influence of parameter uncertainty in multi-criteria decision-making when identifying optimal retrofitting strategies for RC buildings." *J. Earthquake Eng.* (Jun). https://doi.org/10.1080/13632469.2022.2087794.

Carofilis, W., D. Perrone, G. J. O'Reilly, R. Monteiro, and A. Filiatrault. 2020. "Seismic retrofit of existing school buildings in Italy: Performance evaluation and loss estimation." *Eng. Struct.* 225 (Dec): 111243. https://doi.org/10.1016/j.engstruct.2020.111243.

Carofilis Gallo, W. W., G. Gabbianelli, and R. Monteiro. 2021. "Assessment of multi-criteria evaluation procedures for identification of optimal seismic retrofitting strategies for existing RC buildings." *J. Earthquake Eng.* 26 (11): 5539–5572. https://doi.org/10.1080/13632469.2021.1878074.

Caruso, M., R. Pinho, F. Bianchi, F. Cavalieri, and M. Teresa. 2020. "A life cycle framework for the identification of optimal building renovation strategies considering economic and environmental impacts." *Sustainability* 12 (23): 10221. https://doi.org/10.3390/su122310221.

Caterino, N., I. Iervolino, G. Manfredi, and E. Cosenza. 2008. "Multi-criteria decision making for seismic retrofitting of RC structures." *J. Earthquake Eng.* 12 (4): 555–583. https://doi.org/10.1080/13632460701572872.

Clemett, N., W. Carofilis, G. O'Reilly, G. Gabbianelli, and R. Monteiro. 2022. "Optimal seismic retrofitting of existing buildings considering environmental impact." *Eng. Struct.* 250 (Jan): 113391. https://doi.org/10.1016/j.engstruct.2021.113391.

Cosenza, E., C. Del Vecchio, M. Di Ludovico, M. Dolce, C. Moroni, A. Prota, and E. Renzi. 2018. "The Italian guidelines for seismic risk classification of constructions: Technical principles and validation." *Bull. Earthquake Eng.* 16 (12): 5905–5935. https://doi.org/10.1007/s10518-018-0431-8.

Del Vecchio, C., M. Di Ludovico, A. Prota, and G. Manfredi. 2015. "Analytical model and design approach for FRP strengthening of non-conforming RC corner beam–column joints." *Eng. Struct.* 87 (Mar): 8–20. https://doi.org/10.1016/j.engstruct.2015.01.013.

Di Trapani, F., M. Malavisi, G. C. Marano, A. P. Sberna, and R. Greco. 2020. "Optimal seismic retrofitting of reinforced concrete buildings by steel-jacketing using a genetic algorithm-based framework." *Eng. Struct.* 219 (Sep): 110864. https://doi.org/10.1016/j.engstruct.2020.110864.

EDILCLIMA (EDILCLIMA Software and Engineering). 2021. *EC700 Calcolo Prestazioni Energetiche Degli Edifici—Versione 11*. Borgomanero, Italy: EDILCLIMA Software and Engineering.

EnergyPlus. 2022. "The official building simulation program of the United States Department of Energy." Accessed April 11, 2022. https://energyplus.net/.

Eurostat—Electricity Prices. 2021. "Eurostat." Accessed July 27, 2021. https://ec.europa.eu/eurostat/databrowser/view/nrg_pc_205/default/table?lang=en.

Eurostat—Natural Gas Prices. 2021. "Eurostat." Accessed July 27, 2021. https://ec.europa.eu/eurostat/databrowser/view/nrg_pc_203/default/table?lang=en.

Evangelisti, L., C. Guattari, and P. Gori. 2015. "Energy retrofit strategies for residential building envelopes: An Italian case study of an early-50s building." *Sustainability* 7 (8): 10445–10460. https://doi.org/10.3390/su70810445.

Fajfar, P. 2000. "A nonlinear analysis method for performance-based seismic design." *Earthquake Spectra* 16 (3): 573–592. https://doi.org/10.1193/1.1586128.

Falcone, R., F. Carrabs, R. Cerulli, C. Lima, and E. Martinelli. 2019. "Seismic retrofitting of existing RC buildings: A rational selection procedure based on Genetic Algorithms." *Structures* 22 (Dec): 310–326. https://doi.org/10.1016/j.istruc.2019.08.006.

FEMA (Federal Emergency Management Agency). 2018a. *Seismic performance assessment of buildings, volume 1—Methodology.* 2nd ed. Washington, DC: FEMA.

FEMA (Federal Emergency Management Agency). 2018b. *Seismic performance assessment of buildings, volume 3: Supporting electronic materials and background documentation*. 3rd ed. Washington, DC: FEMA.

Formisano, A., G. Vaiano, and F. Fabbrocino. 2019. "Seismic and energetic interventions on a typical South Italy residential building: Cost analysis and tax detraction." *Front. Built Environ.* 5 (Feb): 12. https://doi.org/10.3389/fbuil.2019.00012.

Gabbianelli, G., D. Perrone, E. Brunesi, and R. Monteiro. 2020. "Seismic acceleration and displacement demand profiles of non-structural elements in hospital buildings." *Buildings* 10 (12): 243. https://doi.org/10.3390/buildings10120243.

Gentile, R., and C. Galasso. 2019. *Shedding some light on multi-criteria decision making for seismic retrofitting of RC buildings*. London: Greenwich.

Homewyse. 2021. "Homewyse Material Cost Calculators." Accessed August 12, 2021. https://www.homewyse.com/costs/index.html.

Il Ministro Dello Sviluppo Economico. 2015. *Decreto interministeriale 26 Giugno 2015, Applicazione delle metodologie di calcolo dele prestazioni energetiche e difnizione delle prescrizioni e dei requisti minimi degli edifici*. Rome: Italian Government.

Italian Government. 1993. *D.P.R. 26 agosto 1993, n. 412*. Rome: Italian Government.

Karayannis, C. G., C. E. Chalioris, and G. M. Sirkelis. 2008. "Local retrofit of exterior RC beam–column joints using thin RC jackets—An experimental study." *Earthquake Eng. Struct. Dyn.* 37 (5): 727–746. https://doi.org/10.1002/eqe.783.

Mauro, G., C. Menna, U. Vitiello, D. Asprone, F. Ascione, N. Bianco, A. Prota, and G. Vanoli. 2017. "A multi-step approach to assess the lifecycle economic impact of seismic risk on optimal energy retrofit." *Sustainability* 9 (6): 989. https://doi.org/10.3390/su9060989.

Mazzolani, F. M., A. Formisano, and G. Vaiano. 2018. "Adeguamento sismico di edifici in cemento aramato: BRB e FRP." *Costruzioni metalliche* 1 (Jun): 25–50.

McKenna, F., M. H. Scott, and G. L. Fenves. 2010. "Nonlinear finite-element analysis software architecture using object composition." *J. Comput. Civ. Eng.* 24 (1): 95–107. https://doi.org/10.1061/(ASCE)CP.1943-5487.0000002.

Menna, C., C. Del Vecchio, M. Di Ludovico, G. M. Mauro, F. Ascione, and A. Prota. 2021. "Conceptual design of integrated seismic and energy retrofit interventions." *J. Build. Eng.* 38 (Jun): 102190. https://doi.org/10.1016/j.jobe.2021.102190.

Menna, C., U. Vitiello, G. Mauro, D. Asprone, N. Bianco, and A. Prota. 2019. "Integration of seismic risk into energy retrofit optimization procedures: A possible approach based on life cycle evaluation." In Vol. 290 of *Proc., IOP Conf. Series: Earth and Environmental Science*, 012022. Bristol, UK: IOP Publishing.

metroLED. 2014. "LED vs fluorescent tubes—Comparison in energy consumption, lighting performance & efficiency." Accessed August 12, 2021. https://metroled.ca/led-vs-fluorescent-tubes-comparison-in-energy-consumption-lighting-performance-efficiency/.

Mora, T. D., M. Pinamonti, L. Teso, G. Boscato, F. Peron, and P. Romagnoni. 2018. "Renovation of a school building: Energy retrofit and seismic upgrade in a school building in Motta Di Livenza." *Sustainability* 10 (4): 969. https://doi.org/10.3390/su10040969.

NTC (Norme Tecniche per le Costruzioni). 2018. *Norme Technice Per Le Costruzioni*. Rome: Ministerio Delle Infrastrutture E Dei Trasporti.

O'Reilly, G. J., D. Perrone, M. Fox, R. Monteiro, and A. Filiatrault. 2018. "Seismic assessment and loss estimation of existing school buildings in Italy." *Eng. Struct.* 168 (Aug): 142–162. https://doi.org/10.1016/j.engstruct.2018.04.056.

O'Reilly, G. J., and T. J. Sullivan. 2018. "Quantification of modelling uncertainty in existing Italian RC frames." *Earthquake Eng. Struct. Dyn.* 47 (4): 1054–1074. https://doi.org/10.1002/eqe.3005.

O'Reilly, G. J., and T. J. Sullivan. 2019. "Modeling techniques for the seismic assessment of the existing Italian RC frame structures." *J. Earthquake Eng.* 23 (8): 1262–1296. https://doi.org/10.1080/13632469.2017.1360224.

Passoni, C., A. Marini, A. Belleri, and C. Menna. 2021. "Redefining the concept of sustainable renovation of buildings: State of the art and an LCT-based design framework." *Sustainable Cities Soc.* 64 (Jan): 102519. https://doi.org/10.1016/j.scs.2020.102519.

Perrone, D., G. J. O'Reilly, R. Monteiro, and A. Filiatrault. 2020. "Assessing seismic risk in typical Italian school buildings: From in-situ survey to loss estimation." *Int. J. Disaster Risk Reduct.* 44 (Apr): 101448. https://doi.org/10.1016/j.ijdrr.2019.101448.

Pettinga, D. 2020. "Retrofit of reinforced concrete moment frames in NZ using dual supplemental damping." *Struct. Eng. Int.* 30 (2): 185–191. https://doi.org/10.1080/10168664.2020.1711849.

Pohoryles, D. A., C. Maduta, D. A. Bournas, and L. A. Kouris. 2020. "Energy performance of existing residential buildings in Europe: A novel approach combining energy with seismic retrofitting." *Energy Build.* 223 (Sep): 110024. https://doi.org/10.1016/j.enbuild.2020.110024.

Prota, A., M. Di Ludovico, C. Del Vecchio, and C. Menna. 2020. *Progetto DPC-ReLUIS 2019-2021 WP5: Interventi di rapida esecuzione a basso impatto ed integrati*, 72. Campania, Italy: RELUIS.

Recommended Lighting Levels in Buildings. 2021. "Archtoolbox.com." Accessed July 27, 2021. https://www.archtoolbox.com/materials-systems/electrical/recommended-lighting-levels-in-buildings.html.

Requena-García-Cruz, M.-V., A. Morales-Esteban, P. Durand-Neyra, and J. M. C. Estêvão. 2019. "An index-based method for evaluating seismic retrofitting techniques. Application to a reinforced concrete primary school in Huelva." *PLoS One* 14 (4): e0215120. https://doi.org/10.1371/journal.pone.0215120.

Rosso, F., V. Ciancio, J. Dell'Olmo, and F. Salata. 2020. "Multi-objective optimization of building retrofit in the Mediterranean climate by means of genetic algorithm application." *Energy Build.* 216 (Jun): 109945. https://doi.org/10.1016/j.enbuild.2020.109945.

Saaty, T. L. 1980. *The analytic hierarchy process*. New York: McGraw-Hill.

Sassu, M., F. Stochino, and F. Mistretta. 2017. "Assessment method for combined structural and energy retrofitting in masonry buildings." *Buildings* 7 (3): 71. https://doi.org/10.3390/buildings7030071.

Sassun, K., T. J. Sullivan, P. Morandi, and D. Cardone. 2016. "Characterising the in-plane seismic performance of infill masonry." *Bull. N. Z. Soc. Earthquake Eng.* 49 (1): 98–115. https://doi.org/10.5459/bnzsee.49.1.98-115.

Silva, A., J. M. Castro, and R. Monteiro. 2020. "A rational approach to the conversion of FEMA P-58 seismic repair costs to Europe." *Earthquake Spectra* 36 (3): 1607–1618. https://doi.org/10.1177/8755293019899964.

Sousa, L., and R. Monteiro. 2018. "Seismic retrofit options for non-structural building partition walls: Impact on loss estimation and cost-benefit analysis." *Eng. Struct.* 161 (Apr): 8–27. https://doi.org/10.1016/j.engstruct.2018.01.028.

UNI (Ente Italiano di Normazione). 2008. *Energy performance of buildings: Energy requirements for lighting*. UNI EN 15139:2008. Milan, Italy: UNI.

UNI (Ente Italiano di Normazione). 2014a. *Prestazioni energetiche degli edifici Parte 1: Determinazione del fabbisogno di energia termica dell'edificio per la climatizzazione estiva ed invernale*. UNI/TS 11300-1. Milan, Italy: UNI.

UNI (Ente Italiano di Normazione). 2014b. *Prestazioni energetiche degli edifici Parte 2: Determinazione del fabbisogno di energia primaria per la climatizzazione invernale, per la produzione di acqua calda sanitaria, per la ventilazione e per l'illuminazione in edifici non residenziali*. UNI/TS 11300-2. Milan, Italy: UNI.

UNI (Ente Italiano di Normazione). 2014c. *Prestazioni energetiche degli edifici Parte 4: Utilizzo di energie rinnovabili e di altri metodi di generazione per la climatizzazione invernale e per la produzione di acqua calda sanitaria*. UNI/TS 11300-4. Milan, Italy: UNI.

UNI (Ente Italiano di Normazione). 2016. *Riscaldamento e raffrescamento degli edifici—Dati climatici*. UNI 10349:2016. Milan, Italy: UNI.

WCED (World Commission on Environment and Development). 1987. *Our common future*. United Nations: Brundtland Commission.

Zinzi, M., S. Agnoli, G. Battistini, and G. Bernabini. 2016. "Deep energy retrofit of the T. M. Plauto School in Italy—A five years experience." *Energy Build.* 126 (Aug): 239–251. https://doi.org/10.1016/j.enbuild.2016.05.030.